2010 IEEE International Conference on Robotics and Automation
Anchorage Convention District
May 3-8, 2010, Anchorage, Alaska, USA

Object Caging under Imperfect Shape Knowledge

Peam Pipattanasomporn and Attawith Sudsang

Abstract— **One of the ultimate challenges in robotics is to manipulate an arbitrary object without knowing its exact shape beforehand. The shape is rather acquired on the spot via using a laser range scanner, structure from multiple views; therefore, maybe only partially observed and corrupted by a certain degree of noise. We propose an algorithm to identify available failsafe strategies capable of preventing an object from escaping from the fingers, i.e. caging, even if its shape is partially and/or inaccurately observed. This algorithm extends the previously proposed one that characterizes all caging sets via a maximal dispersion control but, instead of taking a single polytope $\mathcal{P}$ exactly representing the object as input, it takes two polytopes: $\mathcal{P}^+$ and $\mathcal{P}^-$ containing $\mathcal{P}$ and contained in $\mathcal{P}$, respectively. The algorithm characterizes all possible formations of fingers that guarantee to cage any polytope $\mathcal{P}$ such that $\mathcal{P}^- \subseteq \mathcal{P} \subseteq \mathcal{P}^+$ as long as the dispersion (i.e. looseness) of the fingers' formation is kept under a critical value called the maximal dispersion. This allows us to gracefully handle uncertainty of acquired shapes and quickly identify robust solutions in case of simplified shapes.**

I. INTRODUCTION

The problem of object caging was originally posed by Kuperberg [1] as the problem of designing a minimum formation of points to prevent an object from escaping to infinity by any continuous rigid motion. A caged object does not need to be immobilized but must be confined within a bounded region. Studies in caging generally involve attempts to loosely envelope the object by means of simple and robust strategies that tolerate measurement and control noises. In the past few decades, the concept has been applied to various tasks such as grasping and in-hand manipulation [2], [3], [4], [5], [6] motion planning [7], [8] part feeding [9], stable stance computation [10], [11] where manipulators that work as a cage are possibly mobile robots, fingers of grippers, arrays of pins, cylindrical rods, for example.

A field closely related to caging is object grasping. Most high-precision automation require object to be firmly grasped. Computation of grasps aims at finding a configuration that allows the fingers to exert force that can counter balance external forces and torques. This usually relies on sufficient conditions such as force closure and form closure. A comprehensive review on grasping and contact mechanics can be found in [12]. Caging, on the other hand, relies only on geometrical obstruction in order to prevent object from escaping. This offers a relatively large connected set of solutions, namely the *caging set* [2] (or *capture region* [13]). A caging set contains fingers' configurations that once the fingers enter, the object cannot escape as long as the fingers' configuration is maintained to stay inside the set. Error-tolerant grasping [4] can be achieved by tightening the grasp while the finger configuration remains inside a caging set. Similar concept has been applied to part manipulations and stable stance computation [11].

This research is financially supported in part by the Thailand Research Fund through the Royal Golden Jubilee Ph.D. program under grant No. Ph.D. 1.O.CU/51/D.1, the 90^{th} Anniversary of Chulalongkorn University Fund through the Ratchadapiseksomphot Fund, both are greatly appreciated.

P. Pipattanasomporn and A. Sudsang are with Department of Computer Engineering, Chulalongkorn University, Thailand peam@cp27.com, attawith@gmail.com

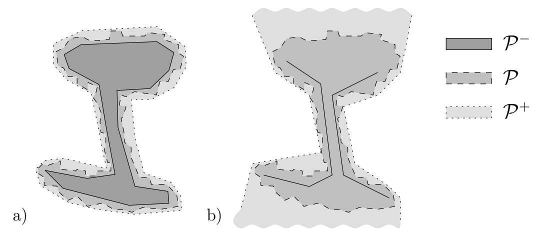

Fig. 1. applications for the proposed algorithm: a) uncertainty of object shape, imperfect rigid body, or approximate solution for complex object b) incomplete shape knowledge.

Given a sufficient number of fingers, caging object on a plane can be achieved by evenly placing fingers in a circle formation surrounding the object. As long as the distance between any pair of adjacent fingers is kept under an upper bound value such as the object's *diameter* [14], or *coverage diameter* [15], the object cannot escape. However, this often leads to inefficient utilization of fingers because two fingers are, in fact, sufficient to cage most objects with concave parts. Rimon and Blake works [2] have laid fundamental concepts in caging and proposed a numerical solution to determine the caging set associated with a given immobilizing grasp of two fingers. Caging with two fingers can be classified by how the separation distance between the two fingers is maintained. One is caging by squeezing fingers: moving the fingers closer together will tighten the cage. The other is caging by stretching fingers: the cage is tighten as the fingers' separation distance increases. Depending on the cage types, the object could not escape if the separation distance is below or above a critical value called the *critical distance*. A critical distance is either *maximal distance* or *minimal distance*. The maximal distance is the greatest distance such that the object cannot escape as long as the fingers' separation is lower than such distance. Conversely, the minimal distance is the smallest distance such that the object cannot escape as long as the fingers' separation exceeds such distance. The maximal and the minimal distance serve as an upper and a lower bound separation distance to maintain the caging by squeezing and stretching, respectively. Vahedi and van der Stappen [16], Pipattanasomporn and Sudsang [17] independently proposed algorithms that report all two-finger caging sets for a given polygonal object. As the number of fingers increases, the problem of reporting all caging sets becomes more complex. One reason is that the caging set associated with a caging configuration can no longer be parameterized by just a critical distance. Erickson et al [13] studied caging convex object with three fingers and proposed both exact and approximate algorithms to render capture region assuming that two fingers are fixed on the boundary of the convex object. Their work was extended to handle non-convex polygon by Vahedi and van der Stappen [18]. Recently, a simplified strategy to cage a polytope with dispersion control was proposed in [19], extending the same strategy applied in two fingers [17], [20] to allow any number of fingers. The idea is to use dispersion as a measure to indicate the looseness of finger formation instead of the separation distance. The condition that the object is caged translates to maintaining the dispersion of the fingers' formation is below the *maximal dispersion* (or above the minimal distance) instead of the maximal (resp. minimal) distance.

To our knowledge, most works related to caging mainly focused on the issues related to inaccurate control and uncertainty in the object's configuration but few have incorporated the problems of uncertainty of object shape resulting from incomplete knowledge, inaccurate observation and/or imperfect rigidity of the object. Such issues undoubtedly arise when a robot need to manipulate an "alien" object, whose shape is not known beforehand and has to be acquired right on the spot via, for example, a range scanner, or structure from multiple views techniques. Moreover, the scanned model are usually overly complex which requires an unreasonable amount of time to report an output, especially for obvious caging formations that can be instantly determined by one's eyeballs. Although, an estimated model can be used as an input to the previously proposed algorithms, reported caging strategies may not guarantee to work with the actual object unknown to the robot. In particular, the algorithm does not incorporate the uncertainty to promise a failsafe baseline, for instance, some reported caging sets may not actually exist and their critical values maybe greater than the correct ones.

In this paper, rather than assuming that a polytope $\mathcal{P}$ representing the actual object shape is known, we assume that we know for certain i) a polytope $\mathcal{P}^+$ that contains $\mathcal{P}$ and ii) a polytope $\mathcal{P}^-$ that was contained in $\mathcal{P}$. Extending from the one in [19], the new algorithm characterizes all the formations that guarantee to cage any bounded polytopes $\mathcal{P}$ such that $\mathcal{P}^- \subseteq \mathcal{P} \subseteq \mathcal{P}^+$ via controlling the formation dispersion below a maximal dispersion. The solution is exactly that of the original algorithm if $\mathcal{P}^- = \mathcal{P} = \mathcal{P}^+$, and naturally degrades if $\mathcal{P}^-$ and $\mathcal{P}^+$ are looser bounds of $\mathcal{P}$. This algorithm works with any finite dimensional workspace and any number of fingers, like in [19], and also functions as a countermeasure to any combinations of the aforesaid problems. Apart from uncertainty in object shape measure, possible applications of the algorithm, shown in Fig. 1.a) and 1.b), are for:

- *Imperfect rigid body:* set $\mathcal{P}^-$, $\mathcal{P}^+$ to bound all shapes resulting from all possible deformation (Fig. 1.a)).
- *Complex object:* set $\mathcal{P}^-$ and $\mathcal{P}^+$ as the simplified polytopes contained by $\mathcal{P}$ and containing $\mathcal{P}$, respectively.
- *Incomplete shape knowledge:* one can set $\mathcal{P}^-$ to be the observed surface of the object while $\mathcal{P}^+$ to be the unobserved or ambiguous region (Fig. 1.b)).

Note that in case of very high shape uncertainty, it is likely that none of formation is the caging formation to all shapes in the family, and the algorithm will not report any caging set.

The paper is organized as follows. In the next section, important results related to caging via controlling maximal dispersion are reintroduced. We then study the important relation between critical dispersion and the object shapes in Section III. In Section IV, we extend to the previously proposed algorithm to report all caging sets containing all caging formations capable of caging any bounded polytope $\mathcal{P}$ with in the family defined by $\mathcal{P}^-$ and $\mathcal{P}^+$. Finally, we conclude and discuss our work in Section V.

II. MAXIMAL DISPERSION CONTROL CAGING

This section review the basics for caging a shape, rigid and exactly known to be a bounded subset $\mathcal{P}$ of η-dimensional space. This shape is to be caged with maximal dispersion control by ϕ point fingers. The shape is possibly not a connected component but all the components must move together as a single rigid body. For convenience, we choose to observe the position of the fingers from the shape's frame of reference, treating the shape as a static obstacle. If the shape is caged under maximal dispersion control, the fingers will not be able to escape to infinity as long as their dispersion is kept below the maximal dispersion. A dispersion is a convex function that maps a formation to a real value i.e. $d : \mathbb{R}^{\eta\times\phi} \rightarrow \mathbb{R}$ such that $d(\mathbf{x}) = d(\mathbf{x}')$ for any $\mathbf{x}$ and $\mathbf{x}'$ having the same formation shape. Note that $\mathbf{x} \equiv (\mathrm{x}_1, \mathrm{x}_2, ..., \mathrm{x}_\phi)$ and $\mathbf{x}'$ have the same formation shape if $\mathbf{x}' = (\mathbf{R}\mathrm{x}_1 + \mathrm{t}, \mathbf{R}\mathrm{x}_2 + \mathrm{t}, ..., \mathbf{R}\mathrm{x}_\phi + \mathrm{t})$ for some $\mathbf{R} \in SO(\eta)$, $\mathrm{t} \in \mathbb{R}^\eta$. Convex function of distances between fingers in the formation are dispersion, for example: $\|\mathrm{x}_1 - \mathrm{x}_2\|^2 + \|\mathrm{x}_2 - \mathrm{x}_3\|^2 + \|\mathrm{x}_3 - \mathrm{x}_2\|^2$; the sum of square distance of between each pair of fingers (supposedly, there are only three of them). Dispersion possesses several properties that later help us simplify the problem. One is that:

Proposition 1: If formations $\mathbf{x}$ and $\mathbf{x}'$ have the same formation shape, their dispersion are not less than that of any formation lies on the line segment $\overline{\mathbf{x}\mathbf{x}'}$

This leads to the fact that: any dispersion attains its minimal value when all the fingers collapse to a single point.

Proposition 2: For any point $\mathrm{x} \in \mathbb{R}^\eta$, a dispersion d attains its minimal value at $(\mathrm{x}, \mathrm{x}, ..., \mathrm{x}) \in \mathbb{R}^{\eta\times\phi}$.

Proof: If η is even, it can be verified that $-\mathbf{I}_\eta \in SO(\eta)$. By Proposition 1, we have that the dispersion of the origin in $\mathbb{R}^{\eta\times\phi}$: $d(\mathbf{0}_{\eta\times\phi}) \leq d(\mathbf{x})$ for any formation $\mathbf{x} \in \mathbb{R}^{\eta\times\phi}$ since $\mathbf{0}_{\eta\times\phi}$ lies at the midpoint between $\mathbf{x}$ and $\mathbf{x}' = -\mathbf{x}$ with $\mathbf{R} = -\mathbf{I}_\eta$, $\mathrm{t} = 0_\eta$.

When η is odd, it can be verified that:

$$\mathbf{A} \equiv \begin{pmatrix} 1 & 0^{\mathrm{T}}_{(\eta-1)} \\ 0_{(\eta-1)} & -\mathbf{I}_{(\eta-1)} \end{pmatrix}, \bar{\mathbf{A}} \equiv \begin{pmatrix} -\mathbf{I}_{(\eta-1)} & 0_{(\eta-1)} \\ 0^{\mathrm{T}}_{(\eta-1)} & 1 \end{pmatrix};$$

are both in $SO(\eta)$. Let $\mathbf{x} \equiv \begin{pmatrix} \mathbf{t} & \mathbf{b} \end{pmatrix}^T, \mathbf{t} \in \mathbb{R}^{1\times\phi}, \mathbf{b} \in \mathbb{R}^{(\eta-1)\times\phi}$. Consider the midpoint $\mathbf{z}$ between $\mathbf{x}$ and $\mathbf{Ax}$:

$$\mathbf{z} \equiv \frac{1}{2}(\mathbf{x} + \mathbf{Ax}) = \frac{1}{2}\begin{pmatrix} \mathbf{t}+\mathbf{t} \\ \mathbf{b}-\mathbf{b} \end{pmatrix} = \begin{pmatrix} \mathbf{t} \\ \mathbf{0}_{(\eta-1)\times\phi} \end{pmatrix},$$

and the midpoint between $\mathbf{z}$ and $\bar{\mathbf{A}}\mathbf{z}$:

$$\frac{1}{2}(\mathbf{z} + \bar{\mathbf{A}}\mathbf{z}) = \frac{1}{2}\begin{pmatrix} \mathbf{t}-\mathbf{t} \\ \mathbf{0}_{(\eta-1)\times\phi} + \mathbf{0}_{(\eta-1)\times\phi} \end{pmatrix} = \mathbf{0}_{\eta\times\phi}$$

Apply Proposition 1 twice to obtain $d(\mathbf{z}) \leq d(\mathbf{x})$ and $d(\mathbf{0}_{\eta\times\phi}) \leq d(\mathbf{z})$. Hence, $d(\mathbf{0}_{\eta\times\phi}) \leq d(\mathbf{x})$ for any $\mathbf{x} \in \mathbb{R}^{\eta\times\phi}$.

It follows from the definition of dispersion that for any $\mathrm{x} \in \mathbb{R}^{\eta}$, the dispersion d attains its minimal value at $\mathbf{x} \equiv (\mathrm{x}, \mathrm{x}, ..., \mathrm{x}) \in \mathbb{R}^{\eta\times\phi}$. ■

When the fingers are at a point they can move together as a single point arbitrarily far from $\mathcal{P}$ if $\mathcal{P}$ is without holes i.e. the compliment of $\mathcal{P}$ is connected. Since the fingers cannot initially reside in any of those holes; otherwise, the shape is trivially caged by placing a finger in a hole, we can safely assume that the compliment of $\mathcal{P}$ is connected.

For convenience, the dispersion function is coupled with the object's shape by setting the dispersion value of a formation to $+\infty$ if the formation is not valid i.e.

$$d_{\mathcal{P}}(\mathbf{x}) = \begin{cases} d(\mathbf{x}), & \mathbf{x} \in (\mathbb{R}^{\eta} \backslash \mathcal{P})^{\phi}; \\ +\infty, & \text{otherwise.} \end{cases}$$

We represent a continuous motion of the fingers' formations with a path in $\mathbb{R}^{\eta\times\phi}$. Concatenation of two paths α and β, written as $\alpha\beta$, is possible if the starting point of β is exactly the end point of α. The reverse of a path α is denoted by α^{-1}. A path that corresponds to a motion that all the fingers eventually reach infinity is called an escape path. Let $\Gamma(\mathbf{x})$ be the set of all escape paths starting from $\mathbf{x}$. The maximal dispersion for a bounded shape $\mathcal{P}$ at a formation $\mathbf{x}$ is given by the least supremum dispersion among all the escape paths starting at $\mathbf{x}$:

$$d^*_{\mathcal{P}}(\mathbf{x}) = \inf_{\alpha\in\Gamma(\mathbf{x})} \left\{ \sup_{\mathbf{y}\in\mathrm{img}(\alpha)} d_{\mathcal{P}}(\mathbf{y}) \right\}.$$

Note that $d_{\mathcal{P}}(\mathbf{x}) \leq d^*_{\mathcal{P}}(\mathbf{x})$ at every $\mathbf{x}$. If $d_{\mathcal{P}}(\mathbf{x}) < d^*_{\mathcal{P}}(\mathbf{x}) < +\infty$, it is possible to control the dispersion d below the maximal dispersion value $d^*_{\mathcal{P}}(\mathbf{x})$; in other words, it is possible to cage the shape $\mathcal{P}$ with the caging formation $\mathbf{x}$ via maximal dispersion control. On the other hand, if $d(\mathbf{x}) = d^*_{\mathcal{P}}(\mathbf{x})$, the shape cannot be caged by maintaining dispersion. For the case that $d^*_{\mathcal{P}}(\mathbf{x}) = +\infty$, either all escape paths from $\mathbf{x}$ are blocked or the fingers cannot eventually keep their formation dispersion finite. In the former situation, we assume that the finger formation cannot cage at such formation $\mathbf{x}$ since some of the fingers cannot initially reach desired positions. The latter is however impossible since $\mathcal{P}$ is bounded. For simplicity, we assume that all shapes referred in the paper are bounded. Clearly, we cannot cage the fingers by maintaining dispersion below a maximal dispersion starting from the formation with minimal dispersion (e.g. when all fingers are at a point by Proposition 2).

Proposition 3: The necessary and sufficient condition that the formation of fingers can certainly cage a shape $\mathcal{P}$ via controlling its formation dispersion below a maximal dispersion starting from a formation $\mathbf{x}$ is: $d(\mathbf{x}) < d^*_{\mathcal{P}}(\mathbf{x}) < +\infty$.

For convenience, a formation is called a caging formation (for $\mathcal{P}$) if it satisfies the condition in Proposition 3.

Our strategy to evaluate $d^*_{\mathcal{P}}(\mathbf{x})$ is based on decomposing the space of all formations $\mathbb{R}^{\eta\times\phi}$ into overlapping convex sets such that $d_{\mathcal{P}}$ restricted on each decomposed convex set is a convex function. Applying Jensen's inequality [21], it follows that:

Proposition 4: Any two formations $\mathbf{x}$, $\mathbf{y}$ in a decomposed convex set are connected by a straight line path α in the set such that $\sup\{d_{\mathcal{P}}(\mathbf{z}) \mid \mathbf{z} \in \mathrm{img}(\alpha)\} = \sup\{d(\mathbf{x}), d(\mathbf{y})\}$.

Since every path connecting $\mathbf{x}$ and $\mathbf{y}$ must include $\mathbf{x}$ and $\mathbf{y}$, the supremum dispersion among all the formations in the straight line path is the least possible among all the paths connecting $\mathbf{x}$ and $\mathbf{y}$.

Assume that the formations $\mathbf{x}$ and $\mathbf{y}$ are contained in two decomposed convex sets C_1 and C_2, respectively. Consider only paths that lie inside $C_1 \cup C_2$ and route from $\mathbf{x}$ to $\mathbf{y}$. Among such paths, we are interested in a path with least supremum dispersion. Observe that each of such paths enter the overlapping region, $C_1 \cap C_2$, before reaching $\mathbf{y}$. Therefore, the least possible supremum dispersion cannot be less than $\sup\{d_{\mathcal{P}}(\mathbf{x}), d_{\mathcal{P}}(\mathbf{m}), d_{\mathcal{P}}(\mathbf{y})\}$ where $\mathbf{m}$ is the formation in $C_1 \cap C_2$ such that $d_{\mathcal{P}}(\mathbf{m}) \leq d_{\mathcal{P}}(\mathbf{z})$ for any $\mathbf{z} \in C_1 \cap C_2$ (if $C_1 \cap C_2$ is empty, $+\infty$ is assumed). Applying Proposition 4, we can construct a path by concatenating two straight line paths: one from $\mathbf{x}$ to $\mathbf{m}$ and the other from $\mathbf{m}$ to $\mathbf{y}$; having the least possible supremum dispersion among paths in $C_1 \cup C_2$. Such path construction can be applied to any sequence of decomposed convex sets. This fact allows us to evaluate the maximal dispersion of a formation by considering all the sequences of decomposed convex sets instead of all the paths from the formation. Those sequences under consideration start from a convex set containing the formation and ends at a convex set containing the formation that all fingers collapse to a point. The maximal dispersion is equivalently the least supremum dispersion of some path induced by one of those sequences.

III. HANDLING SHAPE UNCERTAINTY

In this section, we present theoretical backgrounds for identifying formations that permit us to cage any shapes in a family defined by $\{\mathcal{P} \mid \mathcal{P}^- \subseteq \mathcal{P} \subseteq \mathcal{P}^+\}$. The most important property that let us almost transparently extend previous strategy applied in caging a shape to cage a shape family is that:

Lemma 1: Given that a shape $\mathcal{P}$ that contains another shape $\mathcal{P}^-$, the maximal dispersion for $\mathcal{P}^-$ is everywhere not greater than that for $\mathcal{P}$ i.e. $d^*_{\mathcal{P}^-}(\mathbf{x}) \leq d^*_{\mathcal{P}}(\mathbf{x})$, for any formation $\mathbf{x}$ and $\mathcal{P}^- \subseteq \mathcal{P}$.

Proof: Observe that, for any $\mathcal{P}^- \subseteq \mathcal{P}$, if one or more fingers belongs to the formation $\mathbf{y}$ lie in $\mathcal{P}\backslash\mathcal{P}^-$, $d_{\mathcal{P}^-}(\mathbf{y})$ will be less than $d_{\mathcal{P}}(\mathbf{y})$ as $d_{\mathcal{P}}(\mathbf{y})$ will be set to $+\infty$; otherwise, $d_{\mathcal{P}^-}(\mathbf{y})$ and $d_{\mathcal{P}}(\mathbf{y})$ will have the same value i.e. either equals to $+\infty$ or $d(\mathbf{y})$ depending whether some fingers belongs to the formation $\mathbf{y}$ lie in $\mathcal{P}^-$ or not. This implies that: $d_{\mathcal{P}^-}(\mathbf{y}) \leq d_{\mathcal{P}}(\mathbf{y})$, for any $\mathbf{y}$. Furthermore, for any set of formations, $\mathbf{Y}$: $\sup_{\mathbf{y}\in\mathbf{Y}} d_{\mathcal{P}^-}(\mathbf{y}) \leq \sup_{\mathbf{y}\in\mathbf{Y}} d_{\mathcal{P}}(\mathbf{y})$. Since this applies to image of an arbitrary path, we conclude that $d^*_{\mathcal{P}^-}(\mathbf{x}) \leq d^*_{\mathcal{P}}(\mathbf{x})$. ■

With this fact, we soon arrive at a simple criterion for identifying whether a formation is a caging formation for the shape family or not.

Theorem 1: The necessary and sufficient condition for the fingers to certainly cage any shape $\mathcal{P}$ such that $\mathcal{P}^- \subseteq \mathcal{P} \subseteq \mathcal{P}^+$ via maximal dispersion control starting from a formation $\mathbf{x}$ is: $d(\mathbf{x}) < d^*_{\mathcal{P}^-}(\mathbf{x}) \leq d^*_{\mathcal{P}^+}(\mathbf{x}) < +\infty$.

Proof: ($\Rightarrow$) Since $d(\mathbf{x}) < d^*_{\mathcal{P}^-}(\mathbf{x})$ and, by Lemma 1, $d^*_{\mathcal{P}^-}(\mathbf{x}) \leq d^*_{\mathcal{P}}(\mathbf{x})$ so $d(\mathbf{x}) \leq d^*_{\mathcal{P}}(\mathbf{x})$. Meanwhile, $d^*_{\mathcal{P}^+}(\mathbf{x}) < +\infty$ and, by Lemma 1, $d^*_{\mathcal{P}}(\mathbf{x}) \leq d^*_{\mathcal{P}^+}(\mathbf{x})$ implies that $d^*_{\mathcal{P}}(\mathbf{x}) < +\infty$. Hence, $d(\mathbf{x}) < d^*_{\mathcal{P}}(\mathbf{x}) < +\infty$ which satisfies the condition in Proposition 3. Notice that this proposition just differs slightly from Proposition 3.

($\Leftarrow$) By Lemma 1, $d^*_{\mathcal{P}^-}(\mathbf{x}) \leq d^*_{\mathcal{P}^+}(\mathbf{x})$. What remains to be shown is: if $d^*_{\mathcal{P}^+}(\mathbf{x}) = +\infty$ or $d(\mathbf{x}) = d^*_{\mathcal{P}^-}(\mathbf{x})$, the condition in Proposition 3 will no longer hold for some shape $\mathcal{P}$ such that $\mathcal{P}^- \subseteq \mathcal{P} \subseteq \mathcal{P}^+$. If $d^*_{\mathcal{P}^+}(\mathbf{x}) = +\infty$, the condition in Proposition 3 will not hold for $\mathcal{P} = \mathcal{P}^+$. On the other hand, if $d(\mathbf{x}) = d^*_{\mathcal{P}^-}(\mathbf{x})$, the condition in Proposition 3 will not hold for $\mathcal{P} = \mathcal{P}^-$. ■

Note that we can safely assume that $\mathcal{P}^+$ (and $\mathcal{P}^-$) does not contain any hole (i.e. the compliment of $\mathcal{P}^+$ is connected) since a formation with at least a finger in the hole is considered not reachable. Consequently, the formation is not a caging formation for $\mathcal{P}^+$; therefore, not a caging formation for all the shapes in the family. This means that whether a formation is a caging formation for any shape in the family does not affect even if we fill all the holes of $\mathcal{P}^+$ and $\mathcal{P}^-$. The assumption that the compliment of a shape $\mathcal{P}$ is connected simplifies the condition for $d^*_{\mathcal{P}}(\mathbf{x})$ to be less than infinity. Normally, $d^*_{\mathcal{P}}(\mathbf{x}) < \infty$, if and only if, an escape path from $\mathbf{x}$ that does not overlap with $\mathcal{P}$ exists. However, given the assumption, the condition reduces to: $d^*_{\mathcal{P}}(\mathbf{x}) < +\infty$, if and only if, $d_{\mathcal{P}}(\mathbf{x}) < +\infty$ i.e. non of the fingers belongs to the formation $\mathbf{x}$ is in $\mathcal{P}$. Together with Lemma 1, the caging condition in Theorem 1: $d(\mathbf{x}) < d^*_{\mathcal{P}^-}(\mathbf{x}) \leq d^*_{\mathcal{P}^+}(\mathbf{x}) < +\infty$; reduces to $d(\mathbf{x}) < d^*_{\mathcal{P}^-}(\mathbf{x})$ and $d_{\mathcal{P}^+}(\mathbf{x}) < +\infty$.

Like caging formations for a single shape, a maximally connected set of caging formations of a shape family forms a caging set.

Definition 1: The set of maximally connected caging formation for a shape family containing all $\mathcal{P}$ such that $\mathcal{P}^- \subseteq \mathcal{P} \subseteq \mathcal{P}^+$ is said to be the caging set for the shape family.

It can be implied directly from the definition that any pair of formations: $\mathbf{x}$ and $\mathbf{y}$; are in a caging set for a shape family if they are connected by a path α such that $d(\mathbf{z}) < c$, for some $c < +\infty$ and $d_{\mathcal{P}^+}(\mathbf{z}) < +\infty$, for any $\mathbf{z} \in \text{img}(\alpha)$. What remains to be shown is that the converse is also true. Before that, we need the following proposition:

Proposition 5: Given any two formations $\mathbf{x}$ and $\mathbf{y}$, $d^*_{\mathcal{P}}(\mathbf{x}) = d^*_{\mathcal{P}}(\mathbf{y})$ if there exists a path α from $\mathbf{x}$ to $\mathbf{y}$ such that $\sup\{d_{\mathcal{P}}(\mathbf{z}) \mid \mathbf{z} \in \text{img}(\alpha)\} < d^*_{\mathcal{P}}(\mathbf{y})$.

Proof: Let β (and γ) be the escape path from $\mathbf{x}$ (and $\mathbf{y}$) such that the supremum value of $d_{\mathcal{P}}$ among all formation in its image is exactly $d^*_{\mathcal{P}}(\mathbf{x})$ (and $d^*_{\mathcal{P}}(\mathbf{y})$). The concatenated path $\alpha\gamma$ is an escape path from $\mathbf{x}$ such that $\sup\{d_{\mathcal{P}}(\mathbf{z}) \mid \mathbf{z} \in \text{img}(\alpha\gamma)\} = d^*_{\mathcal{P}}(\mathbf{y})$. This implies that $d^*_{\mathcal{P}}(\mathbf{x}) \leq d^*_{\mathcal{P}}(\mathbf{y})$. However, it is not possible for $d^*_{\mathcal{P}}(\mathbf{x})$ to be less than $d^*_{\mathcal{P}}(\mathbf{y})$; otherwise, $\alpha^{-1}\beta$ forms an escape path from $\mathbf{y}$ such that $\sup\left\{d_{\mathcal{P}}(\mathbf{z}) < d^*_{\mathcal{P}}(\mathbf{y}) \mid \mathbf{z} \in \text{img}(\alpha^{-1}\beta)\right\} < d^*_{\mathcal{P}}(\mathbf{y})$, contradicting the definition of $d^*_{\mathcal{P}}(\mathbf{y})$. ■

Proposition 6: Any two formations $\mathbf{x}, \mathbf{y}$ in a caging set for the shape family defined by $\{\mathcal{P} | \mathcal{P}^- \subseteq \mathcal{P} \subseteq \mathcal{P}^+\}$ are connected by a path α such that, for some $c < +\infty$, $d(\mathbf{z}) < d^*_{\mathcal{P}^-}(\mathbf{z}) = c \leq d^*_{\mathcal{P}^+}(\mathbf{z}) < +\infty$, for any $\mathbf{z} \in \text{img}(\alpha)$.

Proof: Since $\mathbf{x}$ and $\mathbf{y}$ are both in the same caging set, there exists a path from $\mathbf{x}$ to $\mathbf{y}$, say α, such that, for any $\mathbf{z} \in \text{img}(\alpha)$, $d(\mathbf{z}) < d^*_{\mathcal{P}^-}(\mathbf{z}) \leq d^*_{\mathcal{P}^+}(\mathbf{z}) < +\infty$. Let $\mathbf{z}^* \in \text{img}(\alpha)$ such that $d(\mathbf{z}^*) \geq d(\mathbf{z})$ for any $\mathbf{z} \in \text{img}(\alpha)$. Applying Proposition 5 to every formation $\mathbf{z} \in \text{img}(\alpha)$ and $\mathbf{z}^*$ to obtain that $d(\mathbf{z}) < d^*_{\mathcal{P}^-}(\mathbf{z}) = d^*_{\mathcal{P}^-}(\mathbf{z}^*)$. ■

IV. ALGORITHM

From the properties derived in the previous section, we extend the algorithm for exact shapes presented in [19] to support incompleteness and uncertainty. Basically, the the extended algorithm roughly follows the same steps of the previous algorithm, so it is rephrased briefly here:

1) *Partition the workspace* given by $\mathbb{R}^\eta\backslash\mathcal{P}$ into convex subsets: $W_1, W_2, ..., W_n$; such that their union is the workspace itself. We assume for simplicity that boundary of $\mathcal{P}$ is given in the form of $(\eta-1)$-dimensional faces and $W_i \cap W_j$ must be either empty or an $(\eta-1)$-dimensional face belongs to the boundary of $\mathcal{P}$.
2) *Construct the roadmap*, a graph $(\mathbf{V}, \mathbf{E})$ such that $\mathbf{V}$ contains all possible $\phi - 1$ cartesian products among $W_1, W_2, ..., W_n$ and $\mathbf{E}$ contains all intersections between pairs of elements in $\mathbf{V}$ except $\varnothing$. In other words:
$$\begin{aligned} \mathbf{V} &\equiv \left\{W_{i_1} \times W_{i_2} \times ... \times W_{i_\phi}\right\} \\ \mathbf{E} &\equiv \left\{C_1 \cap C_2 \mid C_1, C_2 \in \mathbf{V}\right\} \setminus \{\varnothing\}. \end{aligned}$$
3) *Locate the local minima*. Find a formation with the least dispersion that resides within each vertex and edge. Such task amounts to solving a convex optimization problem. We decorate a set, say X, by underline, $\underline{X}$, to refer to such formation belongs to the set X.
4) *Compute the maximal dispersion*. Let $W_i \times W_i \times ... \times W_i = W_i^\phi \in \mathbf{V}$, for some i, it follows from Proposition 2 that $d^*_{\mathcal{P}}\left(\underline{W_i^\phi}\right)$ is at the global minimum value of dispersion. To obtain the maximal dispersion for all the vertices, the recurrence:
$$d^*_{\mathcal{P}}\left(\underline{C}\right) = \inf_{C \cap C' \in \mathbf{E}} \left\{\sup\left\{d^*_{\mathcal{P}}\left(\underline{C'}\right), d_{\mathcal{P}}\left(\underline{C \cap C'}\right)\right\}\right\};$$

is propagated starting from W_i^ϕ using an algorithm similar to Dijkstra's shortest path, with all vertices except those in the form of W_i^ϕ initially assigned to possess $+\infty$ maximal distance.

5) *Identify caging sets*. If $\underline{C}$ and $\underline{C}'$ are connected by a path whose image is contained in $C \cup C'$ and contains all formations that can guarantee to cage $\mathcal{P}$, C and C' are assigned to the same caging set. Note that this step is not necessary if the user does not need to enumerate caging sets or query them later.

After these steps, the algorithm finishes its job in producing a data structure containing information readied for the following queries.

a) *Query maximal dispersion* at a given formation $\mathbf{x} = (x_1, x_2, ..., x_\phi)$. First, we need to find the graph vertex, say $C_\mathbf{x}$, containing $\mathbf{x}$. $C_\mathbf{x}$ is identified using a point location algorithm [22] by locating the containing convex set W_{i_j} for each finger x_j, $j = 1, 2, ..., \phi$; hence, $C_\mathbf{x} \equiv W_{i_1} \times W_{i_2} \times ... \times W_{i_n}$. Following the Proposition 4, we can evaluate the maximal distance at $\mathbf{x}$: $d^*_\mathcal{P}(\mathbf{x}) = \sup\left\{d_\mathcal{P}(\mathbf{x}), d^*_\mathcal{P}\left(\underline{C_\mathbf{x}}\right)\right\}$.

b) *Query caging set* containing a given formation $\mathbf{x}$. This query performs a step further than a) in that: if $\mathbf{x}$ is known to be a caging formation by checking its formation dispersion against the maximal dispersion. The containing caging set is then reported.

If we neither require to enumerate caging set nor query them, we can just assign $\mathcal{P}$ in the aforesaid steps to $\mathcal{P}^-$, the polytope known for certain to contain the actual shape, instead of the exact one so as to obtain $d^*_{\mathcal{P}^-}$ in step 4) and stop there. The maximal dispersion query can be achieved in exactly the same manner but the given formation $\mathbf{x}$ need to be checked whether it lies in $\mathcal{P}^+$ or not. If it does, $\mathbf{x}$ is not a valid formation for the shape family $\{\mathcal{P} \mid \mathcal{P}^- \subseteq \mathcal{P} \subseteq \mathcal{P}^+\}$. However, for the fully extended version of the algorithm, we need additional tune up. In the original algorithm, a vertex may only overlap with at most one caging set. At the current situation, it is possible that more than one caging sets may appear in a vertex. This causes the algorithm to malfunction at step 5) and when querying a containing caging set.

Assuming that $\mathcal{P}^+$ is an η-dimensional polytope whose boundary is given in the form of $(\eta-1)$-dimensional faces, a simple solution is to force all $(\eta-1)$-dimensional faces of $\mathcal{P}^+$ to appear as a face of some convex polytope W_i. Such partitioning can be achieved via a constrained triangulation/tetrahedronization algorithm. As a result, each W_i is either entirely contained in $\mathcal{P}^+$ or not overlapped with $\mathcal{P}^+$ at all. This implies that, for each vertex $C \in \mathbf{V}$, the fingers forming any formation in C has a fixed number of fingers, denoted by ϕ_C, in the interior of $\mathcal{P}^+$. If ϕ_C is zero, none of the fingers belong to every formation in C are in the interior of shape $\mathcal{P}^+$; otherwise, some of the fingers belong to every formation in C are.

Proposition 7: Each vertex obtained from the proposed partitioning may overlap with at most one caging set for the shape family $\{\mathcal{P} \mid \mathcal{P}^- \subseteq \mathcal{P} \subseteq \mathcal{P}^+\}$.

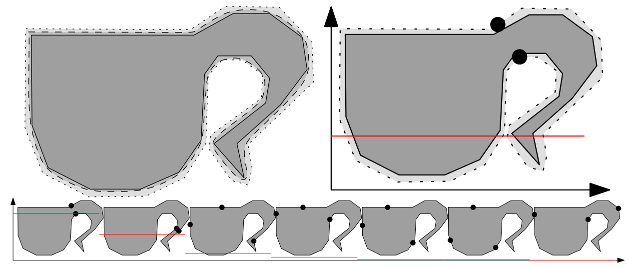

Fig. 2. Polygons with solid outline and dotted outline are $\mathcal{P}^-$ and $\mathcal{P}^+$, respectively, served as bounds for the curved shape $\mathcal{P}$ (dashed outline on the top left). *Top right*: the representative for caging set for the shape family $\{\mathcal{P}|\mathcal{P}^- \subseteq \mathcal{P} \subseteq \mathcal{P}^+\}$. *Bottom*: representatives of each caging set for the shape $\mathcal{P}^-$.

Proof: Let C be a vertex that contains $\mathbf{x}$ and $\mathbf{y}$ from distinct caging sets for the shape family. We assume without loss of generality that $d^*_{\mathcal{P}^-}(\mathbf{x}) \geq d^*_{\mathcal{P}^-}(\mathbf{y})$. Since $\mathbf{x}$ and $\mathbf{y}$ come from distinct caging sets, they are not connected by any path α such that $\sup\{d_{\mathcal{P}^-}(\mathbf{z}) \mid \mathbf{z} \in \mathrm{img}(\alpha)\} < d^*_{\mathcal{P}^-}(\mathbf{x}) < +\infty$. However, Proposition 4 states that there exists a path β from $\mathbf{x}$ to $\mathbf{y}$ such that $\sup\{d_{\mathcal{P}^-}(\mathbf{z}) \mid \mathbf{z} \in \mathrm{img}(\beta)\} = \sup\{d_{\mathcal{P}^-}(\mathbf{x}), d_{\mathcal{P}^-}(\mathbf{y})\}$. Observe that i) $\mathbf{x}$ and $\mathbf{y}$ are in caging sets so $\sup\{d_{\mathcal{P}^-}(\mathbf{x}), d_{\mathcal{P}^-}(\mathbf{y})\} < d^*_{\mathcal{P}^-}(\mathbf{x})$ ii) every formation along β is not in $\mathcal{P}^+$ since $\mathbf{x}, \mathbf{y}$ are not (by the proposed partitioning). This is a contradiction. ∎

The proposed partitioning also leads the condition to identify whether any two adjacent vertices $C, C' \in \mathbf{V}$ are to be assigned to the same caging set (in step 5)). That is: if i) $\phi_C = \phi_{C'} = 0$ and ii) $d(\underline{C}), d(\underline{C}'), d(\underline{C \cap C'})$ are all less than $d^*_{\mathcal{P}^-}(\underline{C}) = d^*_{\mathcal{P}^-}(\underline{C}')$, C, C' are assigned to the same caging set. Since i) implies that the concatenation of straight line paths from $\underline{C}$ to $\underline{C \cap C'}$ and from $\underline{C \cap C'}$ to $\underline{C}'$ does not overlap with $\mathcal{P}^+$ while ii) and Proposition 4 implies that any formation $\mathbf{z}$ in the image of the concatenated path has dispersion less than $d^*_{\mathcal{P}^-}(\underline{C}) = d^*_{\mathcal{P}^-}(\underline{C}')$. By Proposition 6, $\underline{C}$ and $\underline{C}'$ are in the same caging set if i) and ii) hold.

We have implemented and tested the algorithm. The experimental results are shown in Fig. 2, 3 and 4. We perform the experiments on two dimensional workspace with three fingers using the dispersion $d(\mathrm{x}_1, \mathrm{x}_2, \mathrm{x}_3) \equiv \|\mathrm{x}_1 - \mathrm{x}_2\|^2 + \|\mathrm{x}_2 - \mathrm{x}_3\|^2 + \|\mathrm{x}_3 - \mathrm{x}_1\|^2$. Least dispersion formations belong to distinct caging sets are shown in the illustrations. The red lines' altitude above the horizontal axis indicates the square root of difference between the maximal dispersion and the dispersion of the least dispersion formation. For visualization, the red lines' altitude in Fig. 2, 3 and 4 is (resp.) 5, 10 and 5 times of the square root of difference. The results show that caging sets for the shape family $\{\mathcal{P} \mid \mathcal{P}^- \subseteq \mathcal{P} \subseteq \mathcal{P}^+\}$ are significantly smaller (i.e. less difference between the maximal dispersion and the least dispersion formation) than caging sets for a single shape $\mathcal{P}^-$ and some caging sets for $\mathcal{P}^-$ alone are not caging sets for the shape family. In Fig. 4, observe that it is still possible obtain several caging sets for the shape family even if $\mathcal{P}^+$ occupies a large region but not where the fingers should form a caging formation.

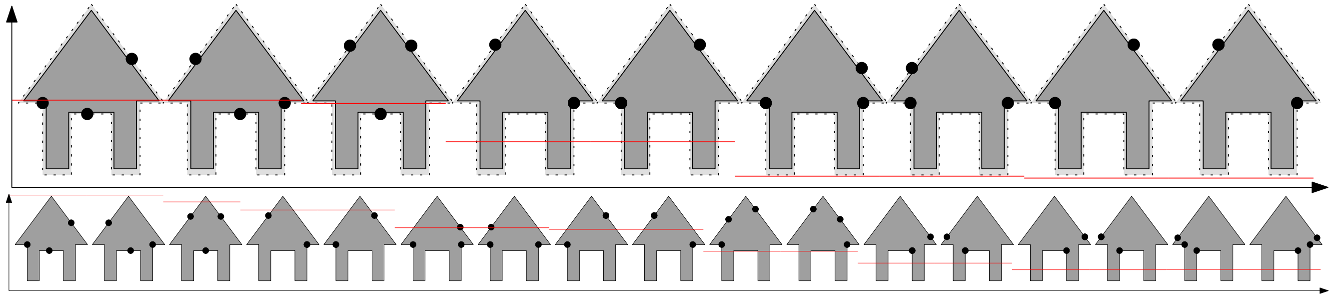

Fig. 3. Polygons with solid outline and dotted outline are $\mathcal{P}^-$ and $\mathcal{P}^+$, respectively. *Top*: representatives of each caging set for the shape family $\{\mathcal{P}|\mathcal{P}^- \subseteq \mathcal{P} \subseteq \mathcal{P}^+\}$. *Bottom*: representatives of each caging set for the shape $\mathcal{P}^-$.

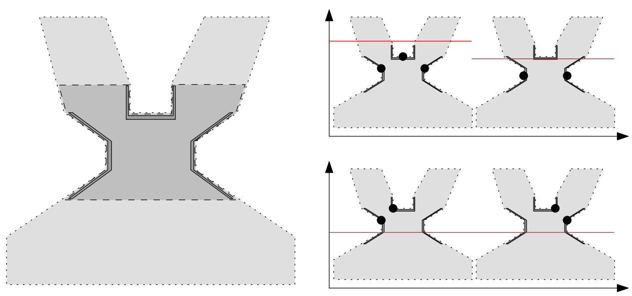

Fig. 4. The region with dotted outlines indicate unobserved region with some degree of uncertainty, P^+. *Left:* dashed region represents the actual shape. *Right:* caging sets of the partially observed shape.

V. CONCLUSIONS AND FUTURE WORKS

The proposed work extend the previous algorithm to handle shape uncertainty. Like the previous algorithm, the caging set for a shape family can be enumerated and queried in the same manner. Although this allows simplification of complex shapes, its workload still increases exponentially with respect to the number of fingers. This still contradicts with one's commonsense that the object should be easier to cage with more fingers. Alternatively, one may cage to the object with a fence of fingers by setting the gap between adjacent fingers less than the coverage diameter as in [15] since time used computing coverage diameter does not depend on the number of fingers. We aim to extend the coverage diameter to support shape uncertainty as well.

REFERENCES

[1] W. Kuperberg, "Problems on polytopes and convex sets," *DIMACS Workshop on Polytopes*, pp. 584–589, January 1990.

[2] E. Rimon and A. Blake, "Caging 2d bodies by 1-parameter two-fingered gripping systems," in *Proceedings of IEEE International Conference on Robotics and Automation*, vol. 2, April 1996, pp. 1459–1464.

[3] C. Davidson and A. Blake, "Caging planar objects with a three-finger one-parameter gripper," in *Proceedings of IEEE International Conference on Robotics and Automation*, vol. 3, May 1998, pp. 2722–2727.

[4] ——, "Error-tolerant visual planning of planar grasp," in *Proceedings of IEEE International Conference on Conference on Computer Vision*, January 1998, pp. 911–916.

[5] K. G. Gopalakrishnan and K. Goldberg, "Gripping parts at concave vertices," in *Proceedings of IEEE International Conference on Robotics and Automation*, vol. 2, pp. 1590–1596.

[6] A. Sudsang, J. Ponce, and N. Srinivasa, "Grasping and in-hand manipulation: Experiments with a reconfigurable gripper," *Advanced Robotics*, vol. 12, no. 5, pp. 509–533, 1997.

[7] A. Sudsang, J. Ponce, M. Hyman, and D. J. Kriegman, "On manipulating polygonal objects with three 2-dof robots in theplane," in *Proceedings of IEEE International Conference on Robotics and Automation*, vol. 3, 1999, pp. 2227–2234.

[8] A. Sudsang, F. Rothganger, and J. Ponce, "Motion planning for disc-shaped robots and pushing a polygonal object in the plane," *IEEE Transactions on Robotics and Automation*, vol. 18, August 2002.

[9] S. J. Blind, C. C. McCullough, S. Akella, and J. Ponce, "Manipulating parts with an array of pins: A method and a machine," *The International Journal of Robotics Research*, vol. 20, no. 10, pp. 808–818, 2001.

[10] D. J. Kriegman, "Let them fall where they may: capture regions of curved objects and polyhedra," *International Journal of Robotics Research*, vol. 16, pp. 448–472, 1997.

[11] E. Rimon, R. Mason, J. W. Burdick, and Y. Or, "A general stance stability test based on stratified morse theory with application to quasi-static locomotion planning," *IEEE Transactions on Robotics*, vol. 24, pp. 626–641, June 2008.

[12] A. Bicchi and V. Kumar, "Robotic grasping and contact: A review," in *Preecedings of IEEE International Conference on Robotics and Automation*, vol. 1, April 2000, pp. 348–353.

[13] J. Erickson, S. Thite, F. Rothganger, and J. Ponce, "Capturing a convex object with three discs," in *Proceedings of IEEE International Conference on Robotics and Automation*, September 2003, pp. 2242–2247.

[14] A. Sudsang, "A sufficient condition for capturing an object in the plane with disc-shaped robots," in *Proceedings of IEEE International Conference on Robotics and Automation*, vol. 1, 2002, pp. 682–687.

[15] P. Vongmasa and A. Sudsang, "Coverage diameters of polygons," in *IEEE/RSJ International Conference on Intelligent Robots and Systems*, p. 4036.

[16] M. Vahedi and A. F. van der Stappen, "Caging polygons with two and three fingers," in *Workshop on the Algorithmic Foundations of Robotics (WAFR) 2006*, July 2006.

[17] P. Pipattanasomporn and A. Sudsang, "Two-finger caging of concave polygon," in *Proceeding of IEEE International Conference on Robotics and Automation*, May 2006, pp. 2137–2142.

[18] M. Vahedi and A. F. van der Stappen, "Caging polygons with two and three fingers," *The International Journal of Robotics Research*, vol. 27, no. 11-12, pp. 1308–1324, 2008.

[19] P. Pipattanasomporn, P. Vongmasa, and A. Sudsang, "Caging rigid polytopes via finger dispersion control," in *Proceeding of IEEE International Conference on Robotics and Automation*, 2008, pp. 1181–1186.

[20] ——, "Two-finger squeezing caging of polygonal and polyhedral object," in *Proceeding of IEEE International Conference on Robotics and Automation*, 2007, pp. 205–210.

[21] S. Boyd and L. Vandenberghe, *Convex Optimization*. Cambridge University Press, 2004, ch. Convex functions, pp. 67–126.

[22] J. Snoeyink, *Handbook of Discrete and Computational Geometry*, 2nd ed. New York: Chapman & Hall/CRC, 2004, ch. 34. Point Location, pp. 767–785.